

A simpler Ramachandran number can simplify the life of a protein simulator

Ranjan V. Mannige^{1,2,*}

¹ KPMG, Atlanta, CA 30309, U.S.A.

² Multiscale Institute, Atlanta, CA 30309, U.S.A.

* ranjanmannige@gmail.com

ABSTRACT

Proteins display complicated structures that often undergo numerous types of structural transformations. Without prior knowledge, it is often difficult to assess exactly where and how regions of a protein structure undergo structural transformation, which often makes it hard to survey new data, such as molecular dynamics trajectories or NMR-derived structural ensembles. Here, we present a suite of protein analysis tools—`plotMAP`—that utilize the Ramachandran number (\mathcal{R}) in various formats in order to succinctly describe features of and dynamics within a new protein ensemble.

INTRODUCTION

Proteins are a class of biomolecules unparalleled in their functionality (Berg *et al.*, 2010). A natural protein may be thought of as a linear chain of amino acids, each normally sourced from a repertoire of 20 naturally occurring amino acids. Proteins are important partially because of the structures that they access: the conformations (conformational ensemble) that a protein assumes determines the functions available to that protein. However, all proteins are dynamic: even stable proteins undergo long-range motions in its equilibrium state; i.e., they have substantial diversity in their conformational ensemble (Mannige, 2014). Additionally, a number of proteins undergo conformational transitions, without which they may not properly function. Finally, some proteins – intrinsically disordered proteins – display massive disorder whose conformations dramatically change over time (Uversky, 2003; Fink, 2005; Midic *et al.*, 2009; Espinoza-Fonseca, 2009; Uversky and Dunker, 2010; Tompa, 2011; Sibille and Bernado, 2012; Kosol *et al.*, 2013; Dunker *et al.*, 2013; Geist *et al.*, 2013; Baruah *et al.*, 2015), and whose characteristic structures are still not well-understood (Beck *et al.*, 2008).

Large-scale changes in a protein occur due to changes in protein backbone conformations. Fig. 1 is a cartoon representation of a peptide/protein backbone, with the backbone bonds themselves represented by darkly shaded bonds. Ramachandran *et al.* (1963) had recognized that the backbone conformational degrees of freedom available to an amino acid (residue) i is almost completely described by only two dihedral angles: ϕ_i and ψ_i (Fig. 1, green arrows). Today, protein structures described in context of the two-dimensional (ϕ, ψ) -space are called Ramachandran plots.

The Ramachandran plot is recognized as a powerful tool for two reasons: 1) it serves as a map for structural ‘correctness’, since many regions within the Ramachandran plot space are energetically not

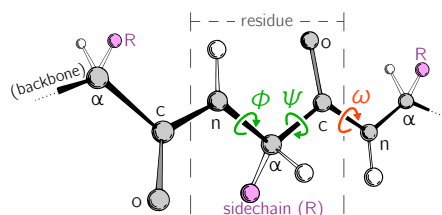


Figure 1. Backbone conformational degrees of freedom dominantly depend on the dihedral angles ϕ and ψ (green), and to a smaller degree depend on the third dihedral angle (ω ; red) as well as bond lengths and angles (unmarked).

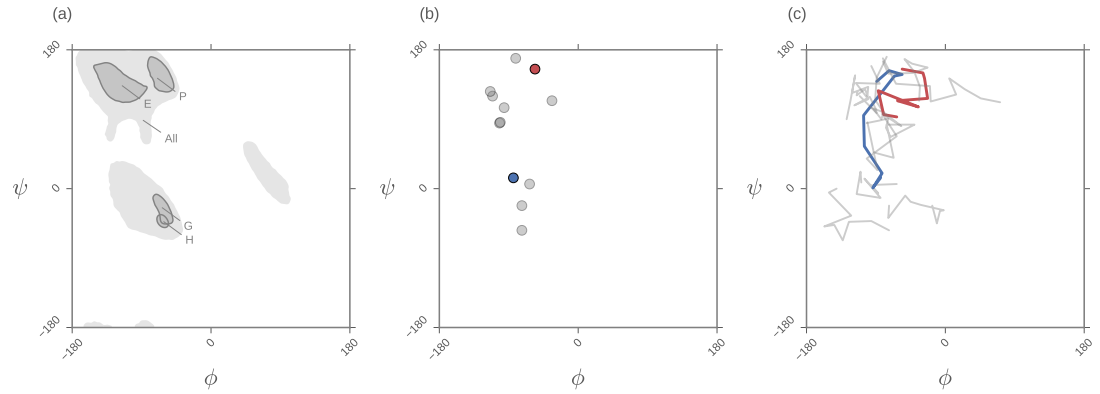


Figure 2. While the Ramachandran plot is useful for exploring peptide backbone structure (a, c), it is not a convenient representation for exploring peptide backbone dynamics (c).

permitted (Momen *et al.*, 2017), allowing ne structures to be interrogated for ‘correctness’ Laskowski *et al.* (1993); Hoof *et al.* (1997); Laskowski (2003); and 2) it provides a snapshot of the structure of a protein (Berg *et al.*, 2010; Alberts *et al.*, 2002; Subramanian, 2001). For example, particular regions within the Ramachandran plot indicate the presence of particular secondary locally-ordered structures such as the α -helix and β -sheet (see Fig. 2a).

While the Ramachandran plot has been useful as a measure of protein backbone conformation, it is not popularly used to assess structural dynamism and transitions (unless specific knowledge exists about whether a particular residue is believed to undergo a particular structural transition). This is because of the two-dimensionality of the plot: describing the behavior of every residue involves tracking its position in two-dimensional (ϕ, ψ) space. For example, a naive description of positions of a peptide in a Ramachandran plot (Fig. 2b) needs more annotations for a per-residue analysis of the peptide backbone’s structure. Given enough residues, it would be impractical to track the position of each residue within a plot. This is compounded with time, as each point in (b) becomes a curve (c), further confounding the situation. The possibility of picking out previously unseen conformational transitions and dynamism becomes a logistical impracticality. As indicated above, this impracticality arises primarily from the fact that the Ramachandran plot is a two-dimensional map.

Consequently, there has been no single compact descriptor of protein structure. This impedes that naïve or hypothesis-free exploration of new trajectories/ensembles. For example, changes in protein trajectory is either comparative or overly holistic: an example of a comparative values is the root mean squared deviation in atomic position (compared, for example, to the the first conformation in the ensemble/trajectory); an example of a holistic metric is the radius of gyration. While these metrics are heavily used by the molecular dynamics community, the change in these metrics over time only provides a general sense that something in the structure is changing. These metrics, however, can not provide any more residue-level details than that. With protein dynamics undergoing a new renaissance – especially due to intrinsically disordered proteins and allostery – having hypothesis-agnostic metrics of protein structure has become even more relevant.

It has recently been shown that the two values (ϕ, ψ) may be conveniently combined into a single number – the Ramachandran *number* $[\mathcal{R}(\phi, \psi)$ or simply $\mathcal{R}]$ – with little loss of information (Mannige *et al.*, 2016). In a previous report, detailed discussions were provided regarding the reasons behind and derivation of \mathcal{R} (Mannige *et al.*, 2016). After briefly reviewing the original closed form of \mathcal{R} , this report provides a simpler version of the equation, and discusses how \mathcal{R} may be used to provide information about protein ensembles and trajectories. Finally, we introduce a software package – `plotMAP` – that can be used by to produce MAPs that describe the behavior of a protein backbone within user-inputted conformations, structural ensembles and trajectories. This package is presently available on GitHub (<https://github.com/ranjanmannige/plotmap.git>).

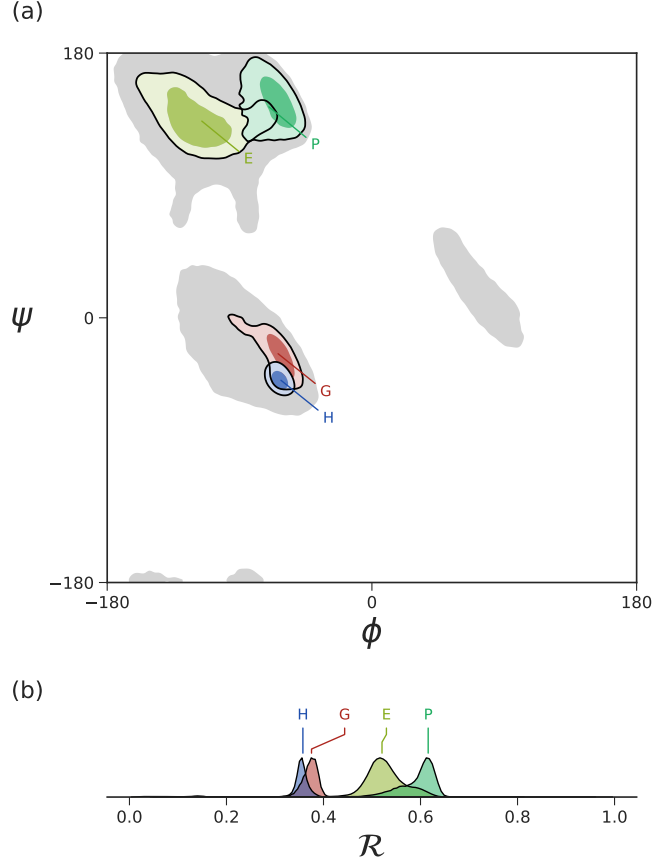


Figure 3. The distribution of dominant regular secondary structures are shown in $[\phi, \psi]$ -space (a) and in \mathcal{R} -space (b). Both Ramachandran plots (a) and Ramachandran ‘lines’ (b) show equivalent resolution of secondary structure, allowing for a more compact representation of Ramachandran plots [Mannige et al. \(2016\)](#).

INTRODUCING THE *SIMPLIFIED* RAMACHANDRAN NUMBER (\mathcal{R})

The Ramachandran number is both an idea and an equation. Conceptually, the Ramachandran number (\mathcal{R}) is any closed form that collapses the dihedral angles ϕ and ψ into one structurally meaningful number ([Mannige et al., 2016](#)). [Mannige et al. \(2016\)](#) presented a version of the Ramachandran number that was complicated in closed form, which poses an impediment in the Ramachandran number utility. Here, for clarity, a much simplified version of the Ramachandran number is discussed, while Section 1.1 shows how this simplified form was derived from the original Ramachandran number equations (Eqns. 3 and 4).

Given arbitrary limits of $\phi \in [\phi_{\min}, \phi_{\max}]$ and $\psi \in [\psi_{\min}, \psi_{\max}]$, where the minimum and maximum values differ by 360° , the most general and accurate equation for the Ramachandran number is

$$\mathcal{R}(\phi, \psi) \equiv \frac{\phi + \psi - (\phi_{\min} + \psi_{\min})}{(\phi_{\max} + \psi_{\max}) - (\phi_{\min} + \psi_{\min})}. \quad (1)$$

For consistency, we maintain throughout this paper that $\phi_{\min} = \psi_{\min} = -180^\circ$, which makes

$$\mathcal{R}(\phi, \psi) = \frac{\phi + \psi + 2\pi}{4\pi}. \quad (2)$$

As evident in Fig. 3, the distributions within the Ramachandran plot are faithfully reflected in corresponding distributions within Ramachandran number space. This paper shows how the Ramachandran number is both compact enough and informative enough to generate immediately useful maps of a dynamic protein.

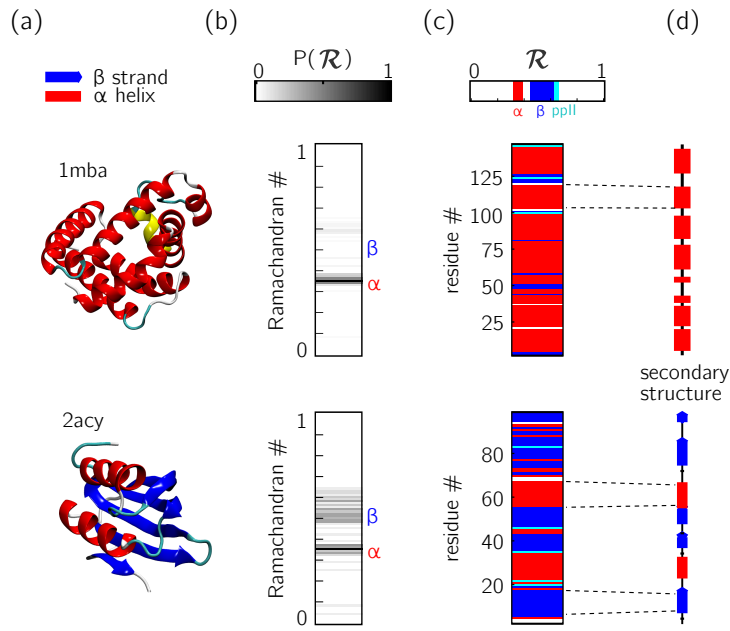


Figure 4. Two types of \mathcal{R} -codes. Digesting protein structures (a) using \mathcal{R} numbers either as histograms (b) or per-residue codes (c) allow for compact representations of salient structural features. For example, a single glance at the histograms indicate that protein 1mba is likely all α -helical, while 2acy is likely a mix of α -helices and β -sheets. Additionally, residue-specific codes (c) not only indicate secondary structure content, but also exact secondary structure stretches (compare to d), which gives a more complete picture of how the protein is linearly arranged.

REASON TO USE THE RAMACHANDRAN NUMBER

Structural motifs are linear/compact

An important aspect of the Ramachandran number (\mathcal{R}) lies in its compactness compared to the traditional Ramachandran pair (ϕ, ψ) . Say we have an N -residue peptide. Then, switching from (ϕ, ψ) to \mathcal{R} appears to only reduce the number of variables from $2N$ to N . However, (ϕ, ψ) values are coupled, i.e., for any N -length peptide, any ordering of $[(\phi_1, \psi_1), (\phi_2, \psi_2), \dots, (\phi_N, \psi_N)]$ can not describe the structure, it is only *pairs* – $[(\phi_1, \psi_1), (\phi_2, \psi_2), \dots, (\phi_N, \psi_N)]$ – that can. Therefore, we must think of switching from (ϕ, ψ) -space to \mathcal{R} -space as a switch in structure space per residue from N two-tuples (ϕ_i, ψ_i) that reside in $\phi \times \psi$ space to N single-dimensional numbers (\mathcal{R}_i).

The value of this conversion is that the structure of a protein can be described in various one-dimensional arrays (per-structure “Ramachandran codes” or “ \mathcal{R} -codes” or simply or “ \mathcal{R} -lines”), which, when arranged vertically/columnarly, constitute easy to digest codes. See, e.g., Fig. 4.

Structural motifs are stackable

In addition to assuming a small form factor, \mathcal{R} -codes may then be *stacked* side-by-side for visual and computational analysis. There lies its true power.

For example, the one- \mathcal{R} -to-one-residue mapping means that the entire residue-by-residue structure of a protein can be shown using a string of \mathcal{R}_i s (which would show regions of secondary structure and disorder, for starters). Additionally, an entire protein’s backbone makeup can be shown as a histogram in \mathcal{R} -space (which may reveal a protein’s topology). The power of this format lies not only in the capacity to distill complex structure into compact spaces, but in its capacity to display *many* complex structures in this format, side-by-side (stacking).

Peptoid nanosheets will be used here as an example of how multiple structures, in the form of \mathcal{R} -codes, may be stacked to provide immediately useful pictograms. Peptoid nanosheets are a recently discovered peptide-mimic that were shown to display a novel secondary structure [Mannige et al. \(2015\)](#). In particular, each peptoid within the nanosheet displays backbone conformations that alternate in chirality, causing the backbone to look like a meandering snake that nonetheless maintains an overall linear direction.

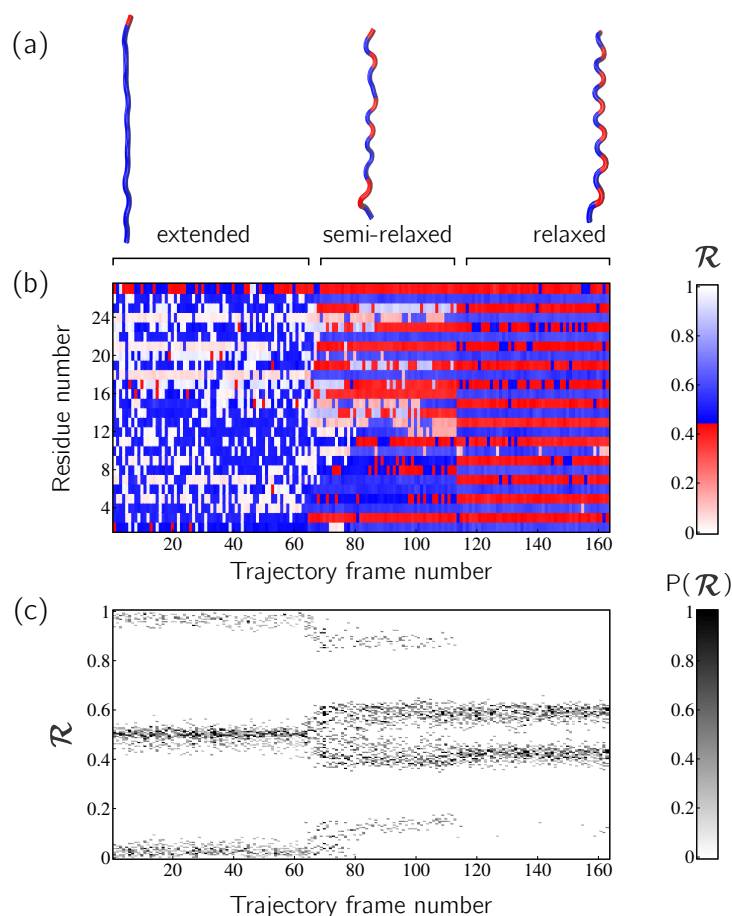


Figure 5. Stacked \mathcal{R} -codes provide useful information at a glance.

107 This secondary structure was discovered by first setting up a nanosheet where all peptoid backbones are
 108 restrained in the extended format (Fig. 5a, left), after which the restraints were energetically softened (a,
 109 middle) and completely released (a, right). As evident in Fig. 5b and Fig. 5c, the two types of \mathcal{R} -code
 110 stacks display salient information at first glance: 1) Fig. 5b shows that the extended backbone first
 111 undergoes some rearrangement with softer restraints, and then becomes much more binary in arrangement
 112 as we look down the backbone (excepting the low-order region in the middle, unshown in Fig. 5a); and
 113 2) Fig. 5c shows that lifting restraints on the backbone causes a dramatic change in backbone topology,
 114 namely a birth of a bimodal distribution evident in the two parallel bands.

115 By utilizing \mathcal{R} , maps such as those in Fig. 5 provide information about every ϕ and ψ within the
 116 backbone. As such, these maps are dubbed MAPs, for Multi Angle Pictures. A Python package called
 117 PlotMAP created Fig. 5a and b, which is provided as a GitHub repository at <https://github.com/ranjanmannige/rnumber>. PlotMAP takes in a PDB structure file containing a single structure, or
 118 multiple structures separated by the code 'MODEL'.
 119

120 **Other uses for \mathcal{R} : picking out subtle differences**

121 As one last example of how \mathcal{R} -numbers may be used to pick out backbone structural trends that would be
 122 hard to decipher by other pictograms. For example, it is well known that prolines (P) display unusual
 123 behavior – in particular while proline backbones occupy structures that are close to but distinct from
 124 α -helical regions. However, due to the two-dimensionality of Ramachandran plots (Fig. 6a), such
 125 distinctions are hard to pick out. However, stacking per-amino-acid \mathcal{R} -codes side by side make such
 126 differences patent.

127 Additionally, it is also known that amino acids preceding prolines display unusual shift in chirality.
 128 For example, Fig. 7 shows that amino acids appearing before prolines and glycines behave much more
 129 differently than they would otherwise. While these results have been discussed previously (Gunasekaran

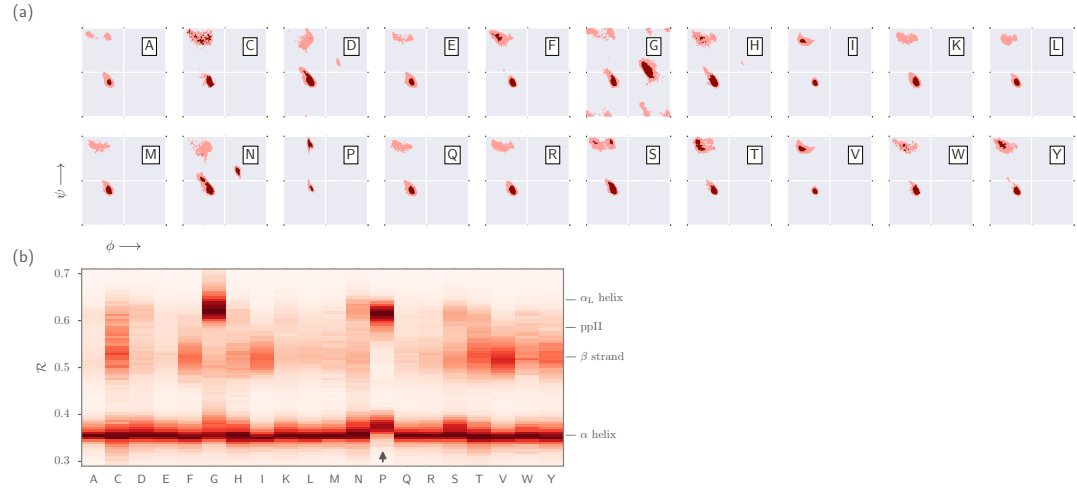


Figure 6. Ramachandran lines are stackable – Part I. Panel (a) shows the per-amino acid backbone behavior of an average protein found in the protein databank (PDB). While these plots are useful, it is difficult to compare such plots. For example, it is hard to pick out the change in the α -helical region of the proline plot (P). However, when we convert Ramachandran plots to Ramachandran *lines* [by converting $(\phi_i, \psi_i) \rightarrow \mathcal{R}_i$], we are able to conveniently “stack” Ramachandran lines calculated for each residue. Then, even visually, it is obvious that proline does not occupy the canonical α -helical region, which is not evident to an untrained eye in (a).

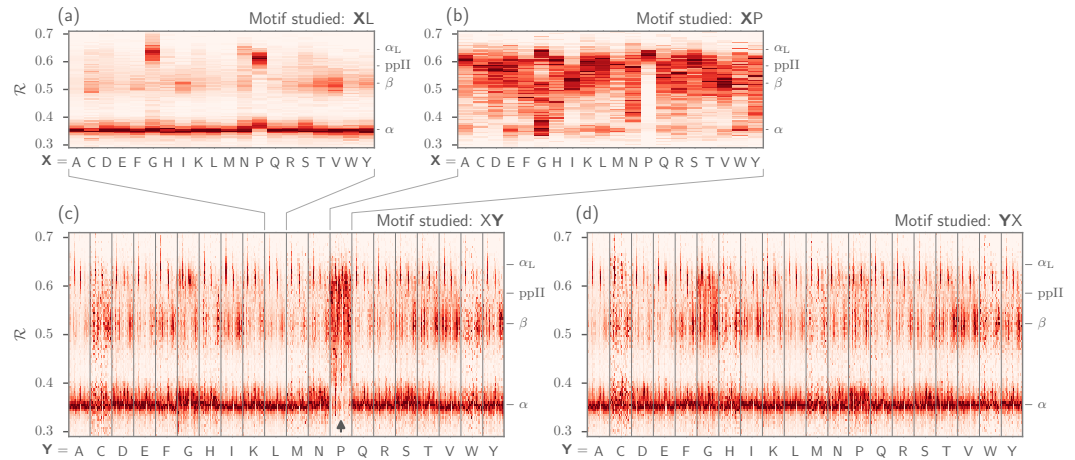


Figure 7. Ramachandran lines are stackable – Part II. Similar to Fig. 6b, Panel (a) represents the behavior of an amino acid ‘Y’ situated *before* a leucine (assuming that we are reading a sequence from the N terminal to the C terminal). Panel (b) similarly represents the behavior of specific amino acids situated before a proline. While residues preceeding a leucine behave similarly to their average behavior (Fig. 6a), most residues preceeding prolines appear to be enriched in structures that change ‘direction’ or backbone chirality ($\mathcal{R} > 0.5$). Panel (c) shows the behavior of individual amino acids when situated before each of the 20 amino acids. This graph shows a major benefit of side-by-side Ramachandran line “stacking”: general trends become much more obvious. For example, it is evident that glycines and prolines dramatically modify the structure of an amino acid preceeding it (compared to average behavior of amino acids in Fig. 6b). This trend is not as strong when considering amino acids that *follow* glycines or prolines (c). Such trends, while previously discovered [e.g., [Gunasekaran et al. \(1998\)](#); [Ho and Brasseur \(2005\)](#)], would not be accessible when naïvely considering Ramachandran plots because one would require 400 (20×20) distinct Ramachandran plots to compare.

130 *et al.*, 1998; Ho and Brasseur, 2005), they were reported more than 30 years after the first structures were
131 published; they would have been relatively easy to find if \mathcal{R} -codes were to be used regularly.

132 The relationships in Figs. 6 and 7 show how subtle changes in structure can be easily picked out when
133 structures are stacked side-by-side in the form of \mathcal{R} -codes. Such subtle changes are often witnessed when
134 protein backbones transition from one state to another.

135 CONCLUSION

136 A simpler Ramachandran number is reported – $\mathcal{R} = (\phi + \psi + 2\pi)/(4\pi)$ – which, while a single num-
137 ber, provides much information. For example, as discussed in Mannige *et al.* (2016), \mathcal{R} values close
138 above 0.5 are left-handed, while those below 0.5 are right handed, \mathcal{R} values close to 0, 0.5 and 1 are
139 extended, β -sheets occupy \mathcal{R} values at around 0.52, right-handed α -helices hover around 0.34. Given
140 the Ramachandran number’s ‘stackability’, single graphs can hold a detailed information of the progres-
141 sion/evolution of molecular trajectories. Finally, a python script (plotMAP.py) has been provided in an
142 online [GitHub repository](#).

143 ACKNOWLEDGMENTS

144 RVM was supported by the Defense Threat Reduction Agency under contract no. IACRO-B0845281.
145 RVM thanks Alana Canfield Mannige for her critique. This work was done at the Molecular Foundry at
146 Lawrence Berkeley National Laboratory (LBNL), supported by the Office of Science, Office of Basic
147 Energy Sciences, of the U.S. Department of Energy under Contract No. DE-AC02-05CH11231.

148 REFERENCES

- 149 **Alberts B, Johnson A, Lewis J, Raff M, Roberts K, Walter P. 2002.** Molecular biology of the cell.
150 new york: Garland science; 2002. *Classic textbook now in its 5th Edition*.
- 151 **Baruah A, Rani P, Biswas P. 2015.** Conformational entropy of intrinsically disordered proteins from
152 amino acid triads. *Scientific reports* 5.
- 153 **Beck DA, Alonso DO, Inoyama D, Daggett V. 2008.** The intrinsic conformational propensities of the
154 20 naturally occurring amino acids and reflection of these propensities in proteins. *Proceedings of the*
155 *National Academy of Sciences* 105(34):12259–12264.
- 156 **Berg JM, Tymoczko JL, Stryer L. 2010.** *Biochemistry, International Edition*. WH Freeman & Co.,
157 New York, 7 edition.
- 158 **Dunker A, Babu M, Barbar E, Blackledge M, Bondos S, Dosztányi Z, Dyson H, Forman-Kay J,
159 Fuxreiter M, Gsponer J, Han KH, Jones D, Longhi S, Metallo S, Nishikawa K, Nussinov R,
160 Obradovic Z, Pappu R, Rost B, Selenko P, Subramaniam V, Sussman J, Tompa P, Uversky V.
161 2013.** What’s in a name? why these proteins are intrinsically disordered? *Intrinsically Disordered*
162 *Proteins* 1:e24157.
- 163 **Espinoza-Fonseca LM. 2009.** Reconciling binding mechanisms of intrinsically disordered proteins.
164 *Biochemical and biophysical research communications* 382(3):479–482.
- 165 **Fink AL. 2005.** Natively unfolded proteins. *Curr Opin Struct Biol* 15(1):35–41.
- 166 **Geist L, Henen MA, Haiderer S, Schwarz TC, Kurzbach D, Zawadzka-Kazimierczuk A, Saxena
167 S, Žerko S, Koźmiński W, Hinderberger D, *et al.* 2013.** Protonation-dependent conformational
168 variability of intrinsically disordered proteins. *Protein Science* 22(9):1196–1205.
- 169 **Gunasekaran K, Nagarajaram H, Ramakrishnan C, Balaram P. 1998.** Stereochemical punctuation
170 marks in protein structures: glycine and proline containing helix stop signals. *Journal of molecular*
171 *biology* 275(5):917–932.
- 172 **Ho BK, Brasseur R. 2005.** The ramachandran plots of glycine and pre-proline. *BMC structural biology*
173 5(1):1.
- 174 **Hooft RW, Sander C, Vriend G. 1997.** Objectively judging the quality of a protein structure from a
175 ramachandran plot. *Computer applications in the biosciences: CABIOS* 13(4):425–430.
- 176 **Kosol S, Contreras-Martos S, Cedeno C, Tompa P. 2013.** Structural characterization of intrinsically
177 disordered proteins by nmr spectroscopy. *Molecules* 18(9):10802–10828.
- 178 **Laskowski RA. 2003.** Structural quality assurance. *Structural Bioinformatics, Volume 44* pages 273–303.
- 179 **Laskowski RA, MacArthur MW, Moss DS, Thornton JM. 1993.** Procheck: a program to check the
180 stereochemical quality of protein structures. *Journal of applied crystallography* 26(2):283–291.

181 **Mannige RV. 2014.** Dynamic new world: Refining our view of protein structure, function and evolution.
182 *Proteomes* **2**(1):128–153.

183 **Mannige RV, Haxton TK, Proulx C, Robertson EJ, Battigelli A, Butterfoss GL, Zuckermann RN,**
184 **Whitelam S. 2015.** Peptoid nanosheets exhibit a new secondary structure motif. *Nature* **526**:415–420.

185 **Mannige RV, Kundu J, Whitelam S. 2016.** The Ramachandran number: an order parameter for protein
186 geometry. *PLoS One* **11**(8):e0160023.

187 **Midic U, Oldfield CJ, Dunker AK, Obradovic Z, Uversky VN. 2009.** Protein disorder in the human
188 diseasome: unfoldomics of human genetic diseases. *BMC Genomics* **10 Suppl 1**:S12. doi:10.1186/
189 1471-2164-10-S1-S12.

190 **Momen R, Azizi A, Wang L, Yang P, Xu T, Kirk SR, Li W, Manzhos S, Jenkins S. 2017.** The role
191 of weak interactions in characterizing peptide folding preferences using a qtaim interpretation of the
192 ramachandran plot (ϕ - ψ). *International Journal of Quantum Chemistry* .

193 **Ramachandran G, Ramakrishnan C, Sasisekharan V. 1963.** Stereochemistry of polypeptide chain
194 configurations. *Journal of molecular biology* **7**(1):95–99.

195 **Sibille N, Bernado P. 2012.** Structural characterization of intrinsically disordered proteins by the
196 combined use of nmr and saxs. *Biochemical society transactions* **40**(5):955–962.

197 **Subramanian E. 2001.** Gn ramachandran. *Nature Structural & Molecular Biology* **8**(6):489–491.

198 **Tompa P. 2011.** Unstructural biology coming of age. *Curr Opin Struct Biol* **21**(3):419–425. doi:
199 10.1016/j.sbi.2011.03.012.

200 **Uversky VN. 2003.** Protein folding revisited. a polypeptide chain at the folding-misfolding-nonfolding
201 cross-roads: which way to go? *Cell Mol Life Sci* **60**(9):1852–1871.

202 **Uversky VN, Dunker AK. 2010.** Understanding protein non-folding. *Biochim Biophys Acta*
203 **1804**(6):1231–1264.

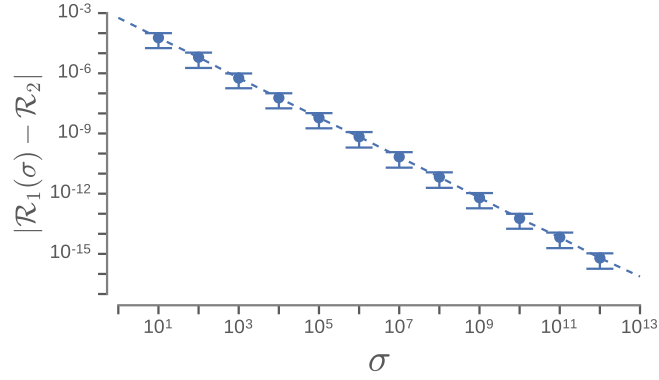


Figure 8. The increase in the accuracy measure (σ) for the original Ramachandran number (Eqn. 4) results in values that tend towards the new Ramachandran number proposed in this paper (Eqn. 5).

1 APPENDIX

1.1 Simplifying the Ramachandran number (\mathcal{R})

This section will derive the simplified Ramachandran number presented in this paper from the more complicated looking Ramachandran number introduced previously [Mannige et al. \(2016\)](#).

Assuming the bounds $\phi, \psi \in [-180^\circ, 180^\circ]$, and the range λ equals 360° , the previously described Ramachandran number takes the form

$$\mathcal{R}(\phi, \psi) \equiv \frac{R_{\mathbb{Z}}(\phi, \psi) - R_{\mathbb{Z}}(\phi_{\min}, \phi_{\min})}{R_{\mathbb{Z}}(\phi_{\max}, \phi_{\max}) - R_{\mathbb{Z}}(\phi_{\min}, \phi_{\min})}, \quad (3)$$

where, $\mathcal{R}(\phi, \psi)$ is the Ramachandran number with range $[0, 1]$, and $R_{\mathbb{Z}}(\phi, \psi)$ is the *unnormalized* integer-spaced Ramachandran number whose closed form is

$$R_{\mathbb{Z}}(\phi, \psi) = \left\lfloor (\phi - \psi + \lambda)\sigma/\sqrt{2} \right\rfloor + \left\lfloor \sqrt{2}\lambda\sigma \right\rfloor \left\lfloor (\phi + \psi + \lambda)\sigma/\sqrt{2} \right\rfloor. \quad (4)$$

Here, $\lfloor x \rfloor$ rounds x to the closest integer value, σ is a scaling factor, discussed below, and λ is the range of an angle in degrees (i.e., $\lambda = \phi_{\max} - \phi_{\min}$). Effectively, this equation does the following. **1)** It divides up the Ramachandran plot into $(360^\circ \sigma^{1/2})^2$ squares, where σ is a user-selected scaling factor that is measured in reciprocal degrees [see Fig. 8b in [Mannige et al. \(2016\)](#)]. **2)** It then assigns integer values to each square by setting the lowest integer value to the bottom left of the Ramachandran plot ($\phi = -180^\circ, \psi = -180^\circ$; green arrow in Fig. 1b) and proceeding from the bottom left to the top right by iteratively slicing down $-1/2$ sloped lines and assigning increasing integer values to each square that one encounters. **3)** Finally, the equation assigns any (ϕ, ψ) pair within $\phi, \psi \in [-\phi_{\min}, \phi_{\max}]$ to the integer value ($R_{\mathbb{Z}}$) assigned to the divided-up square that they exist in.

However useful Eqn. 3 is, the complexity of the equation may be a deterrent towards utilizing it. This paper reports a simpler equation that is derived by taking the limit of Eqn. 3 as σ tends towards ∞ . In particular, when $\sigma \rightarrow \infty$, Eqn. 3 becomes

$$\mathcal{R}(\phi, \psi) = \lim_{\sigma \rightarrow \infty} \mathcal{R}(\phi, \psi) = \frac{\phi + \psi + \lambda}{2\lambda} = \frac{\phi + \psi + 2\pi}{4\pi}. \quad (5)$$

Conformation of this limit is shown numerically in Fig. 8. Since larger σ s indicate higher accuracy, $\lim_{\sigma \rightarrow \infty} \mathcal{R}(\phi, \psi)$ represents an exact representation of the Ramachandran number. Using this closed form, this report will show how both static structural features and complex structural transitions may be identified with the help of Ramachandran number-derived plots.

221 1.2 Other frames of reference

The Ramachandran number shown in Eqn. 5 expects $\phi, \psi \in [-\lambda/2, \lambda/2)$. Given arbitrary limits of $\phi \in [\phi_{\max}, \phi_{\min})$ and $\psi \in [\psi_{\max}, \psi_{\min})$, the most general equation for the Ramachandran number is

$$\mathcal{R}(\phi, \psi) \equiv \frac{\phi + \psi - (\psi_{\min} + \psi_{\min})}{(\psi_{\max} + \psi_{\max}) - (\psi_{\min} + \psi_{\min})}. \quad (6)$$

For example, assuming that $\phi, \psi \in [0, 2\pi)$, the Ramachandran number in that frame of reference will be

$$\mathcal{R}(\phi, \psi)_{\phi, \psi \in [0, 2\pi)} = \frac{\phi + \psi}{4\pi}. \quad (7)$$

222 However, in doing so, the meaning of the Ramachandran number will change. The rest of this manuscript
223 will always assume that all angles range between $-\pi$ (-180°) and π (180°)

224 2 A SIGNED RAMACHANDRAN NUMBER

An additional Ramachandran number – the *signed* Ramachandran number \mathcal{R}_S – is introduced here for backbones that are achiral. \mathcal{R}_S is identical to the original number in magnitude, but which changes sign from $+$ to $-$ as you approach \mathcal{R} numbers that are to the right (or below) the positively sloped diagonal. I.e.,

$$\mathcal{R}_S = \begin{cases} \mathcal{R} & , \text{ if } \psi \geq \phi \\ \mathcal{R} \times -1 & , \text{ if } \psi < \phi \end{cases} \quad (8)$$

225 This metric is important for those glycine-rich peptides (and peptide-mimics such as peptoids) that both
226 left and right regions of the Ramachandran plot; this is because, for such backbones, each $-1/2$ -sloping
227 slide of the Ramachandran plot may intersect more than one relevant region of the Ramachandran plot,
228 which would put two structurally disparate regions within the Ramachandran plot close in \mathcal{R} -space. The
229 signed Ramachandran plot \mathcal{R}_S minimizes the probability of this happening. However, very few residues
230 within structural databases occupy the right side of the Ramachandran plot (3.5%), which means that
231 signed Ramachandran plots would only be useful in special cases (and possibly for IDPs). For this reason,
232 we will proceed below with a focus on the more relevant Ramachandran number \mathcal{R} .